Infotech@Aerospace
26 - 29 September 2005, Arlington, Virginia

AIAA 2005-7067

Coordination of Multiple Micro Air Vehicles Using Consensus Schemes

Wei Ren*

Department of Electrical and Computer Engineering, Utah State University, Logan, UT, 84322, USA

Ella Atkins†

Space Systems Laboratory, University of Maryland, College Park, MD 20742, USA

Micro Air Vehicles (MAVs) will provide a low-cost, redundant means to perform reconnaissance missions in urban or traditional battlefield environments. These miniaturized vehicles, however, will have extremely limited capacity for onboard navigation sensors, processors, and inter-vehicle communication. This paper explores the application of emerging consensus algorithms to the problem of distributed MAV coordination and control. Through the use of local information exchange (sensing or communication) links, MAV teams are able to initialize and maintain controlled formation geometries, effectively forming a sensor web despite the lack of centralized leadership. Results demonstrate the ability of a twenty-MAV team to accurately assemble in a grid formation when all vehicles are initialized in sufficient proximity to enable a (directed) information exchange topology that spans the MAV network. Without such connectivity, MAV sub-groups form, each of which assembles a smaller version of the original grid formation.

I. Introduction

THE Unmanned Air Vehicle (UAV) has become a pervasive technology that enables surveillance with decreased operational cost and less risk to human life than manned vehicle counterparts. A new generation of even more compact Micro Air Vehicles (MAV) is emerging, envisioned to fit in the palm of a soldier's hand and provide over-the-horizon or indoor reconnaissance capabilities.[1] Because size, power, and weight considerations will significantly limit the instrumentation and processing capacity of MAVs, they must achieve robustness as a team rather than as individual vehicles, requiring an alternative approach to traditional guidance, navigation, and control strategies.

Distributed control of multi-vehicle systems has received significant attention in recent years. In some applications of distributed multi-vehicle systems, shared information plays a central role and facilitates the coordination of the group. Often inspired by biological paradigms, in distributed control systems entities organize by sensing only their local environment (e.g., no GPS) and activities of their immediate neighbors (e.g., no network-wide broadcast). A primary challenge for distributed, coordinated control is to design appropriate algorithms such that the group of vehicles can reach *consensus* on the shared information in the presence of limited and unreliable information exchange and dynamically changing interaction topologies as vehicles move in/out of range.

This paper applies consensus theory to the problem of initializing and maintaining an MAV formation given only local information exchange and no global positioning data. A second-order MAV dynamic model is presumed, and results demonstrate the use of consensus to initialize a twenty-vehicle MAV formation that must form a sensor web over a surveillance target area. In this work, a vertical takeoff and landing (VTOL) MAV design is presumed, enabling the formation to hover over its target and perform agile maneuvers as a group. This choice was made to maximize mission design flexibility and to facilitate integration with University of Maryland collaborators developing rotary-wing vehicle and onboard sensor technologies.[2]

*Assistant Professor, Department of Electrical and Computer Engineering, Utah State University, Email: wren@engineering.usu.edu

†Assistant Professor, Department of Aerospace Engineering, University of Maryland, Email: ella@ssl.umd.edu, Senior Member.

II. Problem Statement

A. MAV Equations of Motion

Let (x_i, y_i, h_i), ψ_i, v_i, r_i, and v_{hi} denote the three-dimensional inertial position, heading angle, forward velocity, heading rate, and vertical velocity of the i^{th} rotary-wing micro air vehicle (MAV) respectively. With the rotary-wing MAV equipped with efficient low-level controllers, the simplified equations of motion are given by

$$\begin{aligned}
\dot{x}_i &= v_i \cos(\psi_i) \\
\dot{y}_i &= v_i \sin(\psi_i) \\
\dot{\psi}_i &= r_i \\
\dot{v}_i &= \frac{1}{\alpha_{vi}}(v_i^c - v_i) \\
\dot{r}_i &= \frac{1}{\alpha_{ri}}(r_i^c - r_i) \\
\dot{h}_i &= v_{hi}, \\
\dot{v}_{hi} &= \frac{1}{\alpha_{v_{hi}}}(v_{hi}^c - v_{hi})
\end{aligned} \tag{1}$$

where v_i^c, r_i^c, and v_{hi}^c are the commanded forward velocity, heading rate, and vertical velocity to the low-level controllers, and α_* are positive constants.[3]

To avoid the nonholonomic constraint introduced by Eq. (1), we define

$$\begin{bmatrix} x_{fi} \\ y_{fi} \end{bmatrix} = \begin{bmatrix} x_i \\ y_i \end{bmatrix} + \begin{bmatrix} d_i \cos(\psi_i) \\ d_i \sin(\psi_i) \end{bmatrix}.$$

Note that if (x_i, y_i) represents MAV i's lateral CG position in inertial coordinates, (x_{fi}, y_{fi}) represents the inertial position of a point f_i located a distance d_i along the x body axis of the i^{th} MAV, presuming zero pitch angle. In the following, we will focus on the coordination of (x_{fi}, y_{fi}) instead of (x_i, y_i) to simplify design of the coordination algorithms.

Motivated by Ref. 4, if we let

$$\begin{bmatrix} v_i^c \\ r_i^c \end{bmatrix} = \begin{bmatrix} v_i \\ r_i \end{bmatrix} + \begin{bmatrix} \alpha_{vi} & 0 \\ 0 & \alpha_{ri} \end{bmatrix} \begin{bmatrix} \cos(\psi_i) & -d_i \sin(\psi_i) \\ \sin(\psi_i) & d_i \cos(\psi_i) \end{bmatrix}^{-1} \begin{bmatrix} \mu_{xi} + v_i r_i \sin(\psi_i) + d_i r_i^2 \cos(\psi_i) \\ \mu_{yi} - v_i r_i \cos(\psi_i) + d_i r_i^2 \sin(\psi_i) \end{bmatrix}$$

and

$$v_{hi}^c = v_{hi} + \alpha_{v_{hi}} \mu_{hi},$$

we obtain the following equations of motion:

$$\begin{aligned}
\dot{x}_{fi} &= v_{xi} \\
\dot{v}_{xi} &= \mu_{xi} \\
\dot{y}_{fi} &= v_{yi} \\
\dot{v}_{yi} &= \mu_{yi} \\
\dot{h}_i &= v_{hi} \\
\dot{v}_{hi} &= \mu_{hi}
\end{aligned} \tag{2}$$

Noting that the transformation between $(\mu_{xi}, \mu_{yi}, \mu_{hi})$ and (v_i^c, r_i^c, v_{hi}^c) are invertible, we will focus on the design for control efforts μ_{xi}, μ_{yi}, and μ_{hi} in the following.

B. Information Exchange between MAVs

It is natural to model information exchange between vehicles by directed/undirected graphs. A digraph (directed graph) consists of a pair $(\mathcal{N}, \mathcal{E})$, where $\mathcal{N}$ is a finite nonempty set of nodes and $\mathcal{E} \in \mathcal{N}^2$ is a set

of ordered pairs of nodes, called edges. As a comparison, the pairs of nodes in an undirected graph are unordered. If there is a directed edge from node v_i to node v_j, then v_i is defined as the parent node and v_j is defined as the child node. A directed path is a sequence of ordered edges of the form $(v_{i_1}, v_{i_2}), (v_{i_2}, v_{i_3}), \cdots$, where $v_{i_j} \in \mathcal{N}$, in a digraph. An undirected path in an undirected graph is defined accordingly. A digraph is called strongly connected if there is a directed path from every node to every other node. An undirected graph is called connected if there is a path between any distinct pair of nodes. A directed tree is a digraph, where every node, except the root, has exactly one parent. A directed spanning tree of a digraph is a directed tree formed by graph edges that connect all the nodes of the graph. We say that a graph has (or contains) a directed spanning tree if there exists a directed spanning tree being a subset of the graph. Note that the condition that a digraph has a directed spanning tree is equivalent to the case that there exists a node having a directed path to all the other nodes.

The adjacency matrix $A = [a_{ij}]$ of a weighted digraph is defined as $a_{ii} = 0$ and $a_{ij} > 0$ if $(j, i) \in \mathcal{E}$ where $i \neq j$. The Laplacian matrix of the weighted digraph is defined as $L = [\ell_{ij}]$, where $\ell_{ii} = \sum_{j \neq i} a_{ij}$ and $\ell_{ij} = -a_{ij}$ where $i \neq j$. For an undirected graph, the Laplacian matrix is symmetric positive semi-definite.

III. Consensus Schemes

In this section we review second-order consensus algorithms. Let $\xi_i \in I\!R$ and $\zeta_i \in I\!R$ be the information states of the i^{th} MAV. For example, ξ_i may take the role of x_{fi}, y_{fi}, or h_i while ζ_i may take the role of v_{xi}, v_{yi}, or v_{hi}. Consensus is said to be reached among multiple MAVs if $\|\xi_i(t) - \xi_j(t)\| \to 0$ and $\|\zeta_i(t) - \zeta_j(t)\| \to 0$, $\forall i \neq j$, asymptotically as $t \to \infty$ for any $\xi_i(0)$ and $\zeta_i(0)$.

In Ref. 5, a second-order consensus algorithm is proposed as

$$\begin{aligned} \dot{\xi}_i &= \zeta_i \\ \dot{\zeta}_i &= -\sum_{j=1}^{n} g_{ij} k_{ij} [(\xi_i - \xi_j) + \gamma(\zeta_i - \zeta_j)], \end{aligned} \tag{3}$$

where $k_{ij} > 0$, $\gamma > 0$, $g_{ii} \triangleq 0$, and $g_{ij} = 1$ if information flows from vehicle j to vehicle i and 0 otherwise.

Let $\xi = [\xi_1, \cdots, \xi_n]^T$ and $\zeta = [\zeta_1, \cdots, \zeta_n]^T$. Eq. (3) can be written in matrix form as

$$\begin{bmatrix} \dot{\xi} \\ \dot{\zeta} \end{bmatrix} = \begin{bmatrix} 0_{n\times n} & I_n \\ -L & -\gamma L \end{bmatrix} \begin{bmatrix} \xi \\ \zeta \end{bmatrix}, \tag{4}$$

where $0_{n\times n}$ is the $n \times n$ zero matrix, I_n is the $n \times n$ identity matrix, and $L = [\ell_{ij}]$ is the digraph Laplacian matrix with $\ell_{ii} = \sum_{j \neq i} g_{ij} k_{ij}$ and $\ell_{ij} = -g_{ij} k_{ij}$, $\forall i \neq j$.

As shown in Ref. 5, consensus algorithm (3) achieves consensus asymptotically if the information exchange topology has a (directed) spanning tree (i.e., there exists at least one MAV that can send information directly or indirectly to all the other MAVs in the team) and

$$\gamma > \max_{i=2,\cdots,n} \sqrt{\frac{2}{|\mu_i| \cos(\frac{\pi}{2} - \tan^{-1} \frac{-\text{Re}(\mu_i)}{\text{Im}(\mu_i)})}},$$

where μ_i, $i = 2, \cdots, n$, are the non-zero eigenvalues of $-L$, and $\text{Re}(\cdot)$ and $\text{Im}(\cdot)$ represent the real and imaginary parts of a number respectively.

In one case, it may be desirable that the MAVs preserve a certain formation during their maneuvers. That is, rather than having ξ_i agree on a certain value, we want to have $\xi_i - \tilde{\xi}_{i0}$ reach a common value, denoted as ξ_f^*. As a result, we know that $\xi_i \to \xi_f^* + \tilde{\xi}_{i0}$, where ξ_f^* represents the formation center and $\tilde{\xi}_{i0}$ represents the deviation of each vehicle from the formation center. In this case, we treat $\xi_i - \tilde{\xi}_{i0}$ as the information state of the i^{th} vehicle.

In another case, it may be desirable that ξ_i approaches a constant while ζ_i approaches zero. As a result, we apply the following consensus algorithm:

$$\begin{aligned} \dot{\xi}_i &= \zeta_i \\ \dot{\zeta}_i &= -\alpha\zeta_i - \sum_{j=1}^{n} g_{ij} k_{ij} [(\xi_i - \xi_j) + \gamma(\zeta_i - \zeta_j)], \end{aligned} \tag{5}$$

where $\alpha > 0$. In this case, $\xi_i \to \xi_j$ and $\zeta_i \to \zeta_j \to 0$ as $t \to \infty$.

In addition, if it is desirable that ζ_i approaches $\zeta^d(t)$, we apply the following consensus algorithm:

$$\dot{\xi}_i = \zeta_i$$
$$\dot{\zeta}_i = \dot{\zeta}^d - \alpha(\zeta_i - \zeta^d) - \sum_{j=1}^{n} g_{ij} k_{ij}[(\xi_i - \xi_j) + \gamma(\zeta_i - \zeta_j)], \tag{6}$$

where $\alpha > 0$. In this case, $\xi_i \to \xi_j$ and $\zeta_i \to \zeta_j \to \zeta^d(t)$ as $t \to \infty$.

One novel feature of consensus algorithms (3), (5) and (6) are that they are distributed in the sense that each vehicle only needs information from its (possibly time-varying) local neighbors. In addition, consensus algorithms (3), (5) and (6) allow time-varying uni-directional information exchange, which takes into account measurements from sensors with limited fields of views as well as random data loss for some information exchange links.

IV. Coordination of Multiple MAVs Using Consensus

In this section, we extend the second-order consensus algorithms to coordinate multiple MAVs in the absence of global positioning data, for example, no GPS unit is installed on each vehicle or GPS information is blocked intermittently (e.g., battle field scenario). The MAVs are driven from their initial locations on a desired heading. During their maneuvers, local neighboring MAVs are required to preserve a certain distance between each other and avoid collisions with each other with only relative information available. The tasks of formation keeping and collision avoidance will be achieved via distributed communication or sensing in that each MAV may only be able to interact with neighboring MAVs that are within communication/sensing range.

We propose the following control law for μ_{hi} as

$$\mu_{hi} = -\alpha_h v_{hi} - \sum_{j=1}^{n} g_{ij} k_{ij}[(h_i - h_j) + \gamma_h(v_{hi} - v_{hj})], \tag{7}$$

where $\alpha_h > 0$, $k_{ij} > 0$, $\gamma_h > 0$, the first term is used to guarantee that $v_{hi} \to 0$, and the second term is applied to guarantee that $\|h_i - h_j\| \to 0$ and $\|v_{hi} - v_{hj}\| \to 0$. Control law (7) guarantees that each MAV aligns its altitude with its local neighbors in a distributed manner.

Let $d_{ij} = \sqrt{(x_{fi} - x_{fj})^2 + (y_{fi} - y_{fj})^2}$. Let d_{sep} represent a desired lateral separation distance between two neighboring MAVs. Let $r_i = [x_{fi}, y_{fi}]^T$. We define a continuous function $\phi(d_{ij})$ such that $\phi = 0$ when $d_{ij} = d_{sep}$, $\phi > 0$ when $d_{ij} > d_{sep}$, $\phi < 0$ when $2r_s < d_{ij} < d_{sep}$, and $\phi \to -\infty$ when $d_{ij} \to 2r_s$, where $\{\rho | \, \|\rho - r_i\| \leq r_s\}$ defines the safe region of each MAV. Also let (v_x^d, v_y^d) be the desired group velocity for the whole team represented in the inertial x-y plane. Motivated by Refs. 4,6–9, we propose the following control laws for μ_{xi} and μ_{yi}.

$$\mu_{xi} = \dot{v}_x^d - \alpha_x(v_{xi} - v_x^d) - \sum_{j=1}^{n} g_{ij}\gamma_x(v_{xi} - v_{xj}) - \sum_{j=1}^{n} g_{ij}\beta_x\phi(d_{ij})(x_{fi} - x_{fj}) \tag{8}$$

$$\mu_{yi} = \dot{v}_y^d - \alpha_y(v_{yi} - v_y^d) - \sum_{j=1}^{n} g_{ij}\gamma_y(v_{yi} - v_{yj}) - \sum_{j=1}^{n} g_{ij}\beta_y\phi(d_{ij})(y_{fi} - y_{fj}) \tag{9}$$

where $\alpha_x > 0$, $\alpha_y > 0$, $\beta_x > 0$, $\beta_y > 0$, $\gamma_x > 0$, and $\gamma_y > 0$. The first two terms in Eqs. (8) and (9) are used to guarantee that (v_{xi}, v_{yi}) approaches (v_x^d, v_y^d), the third terms in Eqs. (8) and (9) are used to guarantee that $|v_{xi} - v_{xj}| \to 0$ and $|v_{yi} - v_{yj}| \to 0$, and the fourth terms in Eqs. (8) and (9) are used to achieve collision avoidance and maintain d_{sep} between each neighboring MAV pair.

In contrast to Refs. 4,7–9, where bi-directional information exchange is required, the information exchange topology may be uni-directional in Eqs. (7), (8), and (9) to account for measurements from sensors with limited fields of views, random information loss, or delayed data transmission (e.g., to save power). Control laws (7), (8), and (9) can guarantee formation maintenance of a team of MAVs if at each time there exists at least one MAV that can send information directly or indirectly to all the other MAVs in the team and γ_x, γ_y, and γ_h are sufficiently large.

As two examples of $\phi(\cdot)$, let $\phi_1(d_{ij}) = \log(\frac{d_{ij}-2r_s}{d_{sep}-2r_s})$ and $\phi_2(d_{ij}) = \log(\frac{\text{sat}(d_{ij}-2r_s,\epsilon_s,\infty)}{d_{sep}-2r_s})$, where ϵ_s is a small positive number and $\text{sat}(\cdot,\cdot,\cdot)$ is defined as

$$\text{sat}(a,b,c) = \begin{cases} b, & a < b \\ a, & b \le a \le c \\ c, & a > c \end{cases},$$

where it is assumed that $b < c$. Fig. 1 shows a plot of $\phi_1(d_{ij})$ and $\phi_2(d_{ij})$, where $d_{sep} = 8$ meters, $r_s = 0.5$ meters, and $\epsilon_s = 0.001$ meters. Note that $\phi_2(\cdot)$ assumes a finite repulsive force when two MAVs move sufficiently close.

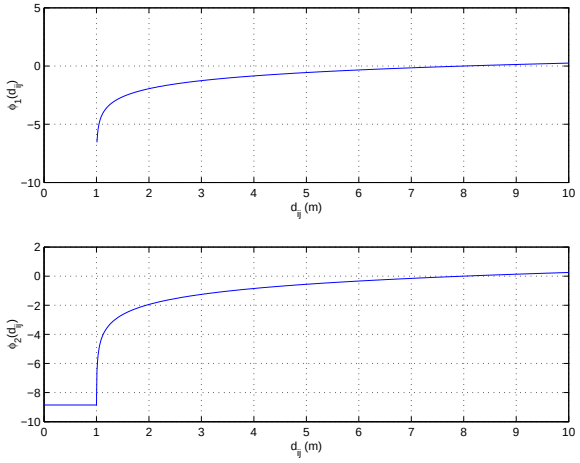

Figure 1. Plot of $\phi_1(d_{ij})$ and $\phi_2(d_{ij})$ with respect to d_{ij}.

V. Simulation Results

In this section, we simulate a scenario where twenty MAVs are controlled to form a sensor web using control laws (7), (8), and (9). The parameter values used in the simulation are given by Table 1. In this paper, we assume that each MAV has a limited communication/sensing range R. We also assume that each MAV has a safe region defined by $\{\rho | \, \|\rho - r_i\| \le r_s\}$. As illustrated in Fig. 2, each MAV can only communicate with or sense neighboring MAVs that are within R of the current MAV. Note that each MAV's nearest neighbors may be time-varying as MAVs move around. Taking into account measurements from sensors with limited fields of views or random communication data loss, we assume that it is possible that the i^{th} MAV can obtain information from the j^{th} MAV but not vice versa at a certain time. That is, the communication/sensing graph is generally bi-directional but may be sporadically uni-directional over one or more time steps. In the following we assume that at each time step 10% of the existing information exchange links fail, which implies that the communication/sensing graph may be uni-directional at some time steps.

We will consider six cases. In the first and third cases, the initial configuration of the MAVs forms a grid, where the distance between two neighboring MAVs along the x-axis is chosen randomly from $[6, 7]$ meters and the distance between two neighboring MAVs along the y-axis is chosen randomly from $[9, 10]$ meters. The initial altitude of each MAV is chosen randomly from $[100, 110]$ meters. In the other four cases, the initial (x, y) coordinates of each MAV are chosen randomly and the initial altitudes are chosen randomly from $[100, 110]$ meters. Table 2 shows the parameters specific for each case.

In the following we use squares and circles to represent the initial and final positions of each MAV respectively. In Case 1, Fig. 3 shows the configuration of the MAVs in 3D at $t = 0$ and $t = 60$ seconds. Fig. 4 shows the locations of the MAVs in x-y plane while Fig. 5 shows the altitudes of four MAVs. Note that the distance between neighboring MAVs converges to the 8 meter value and the altitude of each MAV reaches a common value. Fig. 6 shows the commanded forward velocities, heading rates, and vertical velocities of four MAVs. Note that the control commands satisfy the saturation constraints defined in Table 1.

Table 1. Parameter values used in simulation.

Parameter	Value
α_{vi}	1
α_{ri}	1
$\alpha_{v_{hi}}$	1
k_{ij}	1
$\alpha_x, \alpha_y, \alpha_h$	2
$\gamma_x, \gamma_y, \gamma_h$	2
β_x, β_y	$\frac{5}{d_{ij}+0.01}$
v_i^c	$\in [-1, 1]$ m/s
r_i^c	$\in [-1, 1]$ rad/s
v_{hi}^c	$\in [-0.5, 0.5]$ m/s
v_x^d	$\frac{\sqrt{2}}{2}$ m/s
v_y^d	$\frac{\sqrt{2}}{2}$ m/s
r_s	0.5 m

Table 2. Control parameters for different cases.

Case 1, 2	$t \in [0, 60]$ sec	$R = 10$ m	$d_{sep} = 8$ m
Case 3	$t \in [0, 80]$ sec	$R = 10$ m	$d_{sep} = 8$ m
Case 4, 5	$t \in [0, 80]$ sec	$R = 20$ m	$d_{sep} = 8$ m
Case 6	$t \in [0, 120]$ sec	$R = 20$ m	$d_{sep} = 8$ m, $t \in [0, 80)$; $d_{sep} = 10$ m, $t \in [80, 120]$

In Case 2, Fig. 7 shows the configuration of the MAVs in 3D at $t = 0$ and $t = 60$ seconds. Fig. 8 shows the locations of the MAVs in the x-y plane while Fig. 9 shows the altitudes of four MAVs. From Fig. 8, we can see that the MAVs form two separated subgroups at $t = 0$ in the sense that MAVs #16, #17, #18, #19, denoted as subgroup 1, have no information exchange with the other MAVs, denoted as subgroup 2, in the team. As a result, two separate subgroups are formed with the distance between neighboring MAVs in each subgroup converging to the 8 meter value. In addition, the altitudes of subgroup 1 reach a common value while the altitudes of subgroup 2 reach another common value. Fig. 10 shows the commanded forward velocities, heading rates, and vertical velocities of four MAVs. Note that the control commands satisfy the saturation constraints defined in Table 1.

In the following we only show locations of each MAV in the x-y plane for simplicity. In Case 3, we assume that MAV #4 and #13 fail when $t \geq 40$ seconds. Fig. 11 shows the locations of the MAVs in the x-y plane at $t = 0$ and $t = 80$ seconds. Note that the remaining MAVs in the team are reorganized and still preserve the desired 8 meter separation distance between neighboring MAVs after MAV #4 and #13 dropped out of the formation.

In Case 4, we assume that the communication/sensing range R is increased to be 20 meters. Fig. 12 shows the locations of the MAVs in the x-y plane at $t = 0$ and $t = 80$ seconds. Note that the desired 8 meter separation distance between neighboring MAVs is not preserved although the MAVs still form a sensor web. This is due to the fact that $R \gg d_{sep}$ and the team of MAVs reaches a local minimum.

In Case 5, we still assume that $R = 20$ meters. However, rather than exchanging information with neighbors that are within its communication/sensing range, each MAV only exchanges information with its nearest neighbors. Fig. 13 shows the locations of the MAVs in the x-y plane at $t = 0$ and $t = 80$ seconds. Note that the desired 8 meter separation distance between neighboring MAVs is preserved even if $R \gg d_{sep}$. However, separated subgroups may occur as shown in Fig. 13.

In Case 6, we still assume that $R = 20$ meters. At $t \in [0, 40)$ seconds, each MAV exchanges information with neighbors that are within its communication/sensing range. At $t \in [40, 120]$ seconds, each MAV

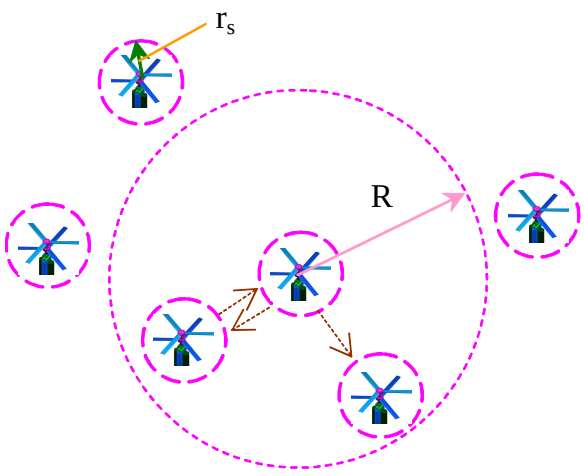

Figure 2. Communication/sensing relationship between neighboring MAVs.

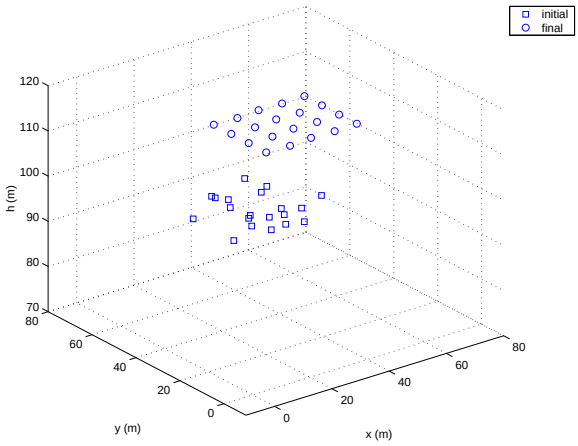

Figure 3. Locations of each MAV in 3D at $t = 0$ sec and $t = 60$ sec in Case 1

exchanges information with its nearest neighbors. Also at $t \in [80, 120)$ the desired separation distance between neighboring MAVs is increased from 8 meters to 10 meters. Fig. 14 shows the locations of the MAVs in the x-y plane at $t = 0, 40, 80, 120$ seconds. Unlike in Case 5, the issue of separated subgroups is avoided since we require the team of MAVs to aggregate at the beginning ($t \in [0, 40)$ seconds) and then use information exchange with nearest neighbors to achieve the desired separation distance. Note that the desired 8 meter separation distance between neighboring MAVs is preserved at $t = 80$ seconds while the desired 10 meter separation distance between neighboring MAVs is preserved at $t = 120$ seconds.

VI. Conclusion

This paper has applied second-order consensus algorithms to the task of coordinating Micro Air Vehicles (MAVs) in a distributed fashion given limited communication/sensing capabilities. The twenty-MAV team deployed in our simulations illustrates the system's capability to initialize formations provided the vehicles are initially arranged such that they form a (directed) network connecting all MAVs at least indirectly.

Although we have only presented results from formation initialization, our simulator can straightforwardly maintain the formation long-term provided injected navigation sensor and communication link noise levels are not prohibitively high. The simple second-order model of vehicle dynamics was derived from a controlled

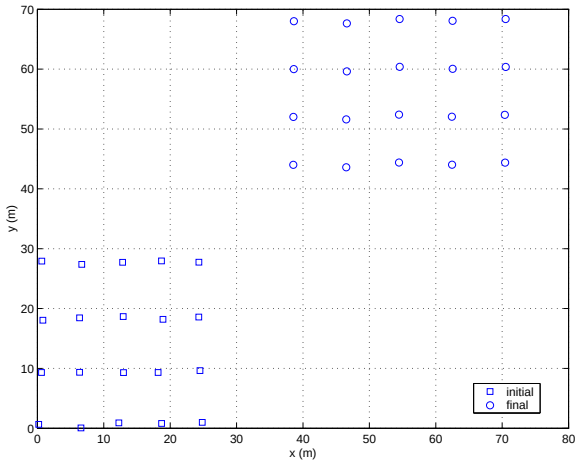

Figure 4. Locations of each MAV in x-y plane at $t = 0$ sec and $t = 60$ sec in Case 1.

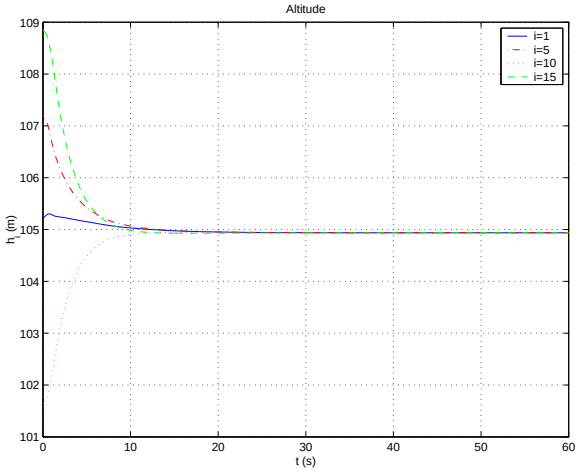

Figure 5. MAV altitudes in Case 1.

UAV helicopter. However, it is somewhat idealistic to presume, particularly since MAV sensors are likely to provide less precise vehicle control capabilities. As more realistic MAV sensor and dynamics models become available, it is expected that consensus algorithms can not only organize a formation in a distributed fashion, but they may also act as a filter over multiple vehicle datasets such that the team flies along a smooth trajectory despite the limited sensor capabilities onboard each MAV.

Acknowledgments

This research is supported by the Army Research Office through the MAV MURI Program (Grant No. ARMY-W911NF0410176) with Technical Monitor as Dr. Gary Anderson.

References

[1]Arning, R. K. and Sassen, S., "Flight Control of Micro Aerial Vehicles," *Proceedings of the AIAA Guidance, Navigation, and Control Conference*, Providence, Rhode Island, August 2004, (AIAA 2004-4911).

[2]Bohorquez, F. and Pines, D., "Hover Performance of Rotor Blades at Low Reynolds Numbers for Rotary Wing Micro Air Vehicles," *Proceedings of the 2nd AIAA Unmanned Unlimited Conference*, San Diego, CA, September 2003, (AIAA 2003-6655).

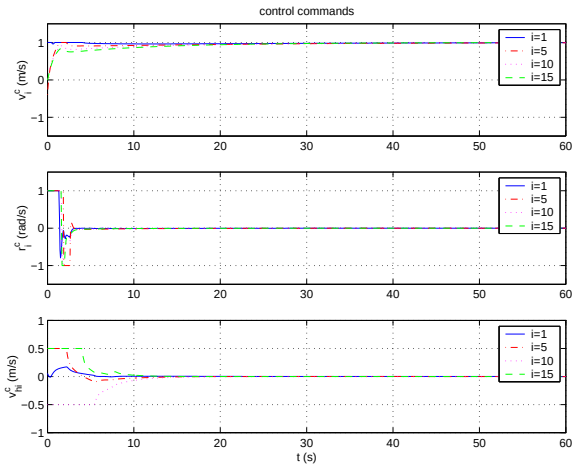

Figure 6. MAV control commands in Case 1.

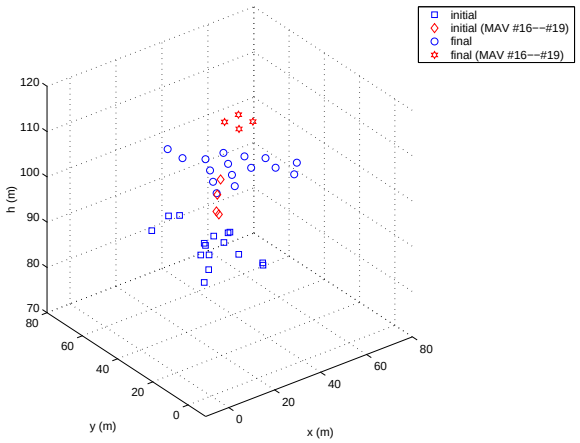

Figure 7. Locations of each MAV in 3D at $t = 0$ sec and $t = 60$ sec in Case 2.

[3]Gavrilets, V., Mettler, B., and Feron, E., "Human-Inspired Control Logic for Automated Maneuvering of Miniature Helicopter," *AIAA Journal of Guidance, Control, and Dynamics*, Vol. 27, No. 5, September–October 2004, pp. 752–759.

[4]Lawton, J. R., Beard, R. W., and Young, B., "A Decentralized Approach To Formation Maneuvers," *IEEE Transactions on Robotics and Automation*, Vol. 19, No. 6, December 2003, pp. 933–941.

[5]Ren, W. and Atkins, E., "Second-order Consensus Protocols in Multiple Vehicle Systems with Local Interactions," *Proceedings of the AIAA Guidance, Navigation, and Control Conference*, San Francisco, CA, August 2005, Paper No. AIAA-2005-6238.

[6]Leonard, N. E. and Fiorelli, E., "Virtual Leaders, Artificial Potentials and Coordinated Control of Groups," *Proceedings of the IEEE Conference on Decision and Control*, Orlando, Florida, December 2001, pp. 2968–2973.

[7]Tanner, H. G., Jadbabaie, A., and Pappas, G. J., "Stable Flocking of Mobile Agents, Part I: Fixed Topology," *Proceedings of the IEEE Conference on Decision and Control*, Maui, Hawaii, December 2003, pp. 2010–2015.

[8]Tanner, H. G., Jadbabaie, A., and Pappas, G. J., "Stable Flocking of Mobile Agents, Part I: Dynamic Topology," *Proceedings of the IEEE Conference on Decision and Control*, Maui, Hawaii, December 2003, pp. 2016–2021.

[9]Olfati-Saber, R., "Flocking for Multi-Agent Dynamic Systems: Algorithms and Theory," *IEEE Transactions on Automatic Control*, 2004, (submitted).

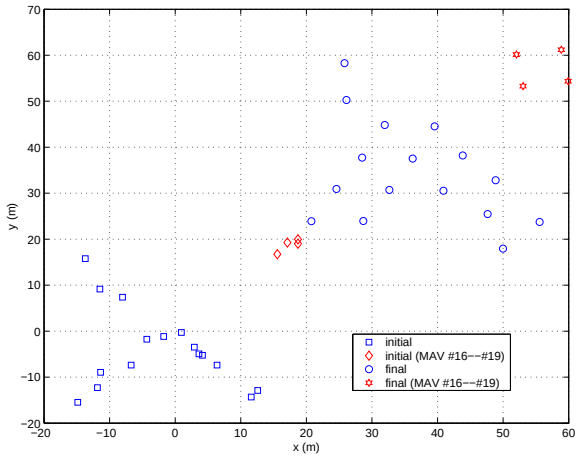

Figure 8. Locations of each MAV in x-y plane at $t = 0$ sec and $t = 60$ sec in Case 2.

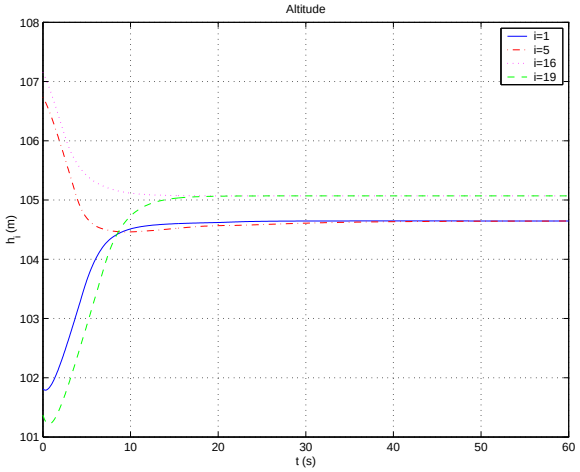

Figure 9. MAV altitudes in Case 2.

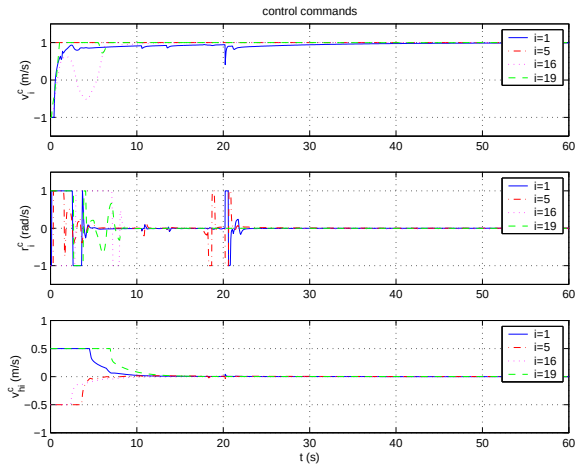

Figure 10. MAV control commands in Case 2.

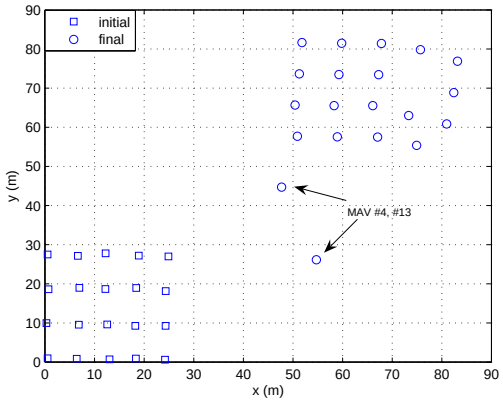

Figure 11. Locations of each MAV in x-y plane at $t = 0$ sec and $t = 80$ sec in Case 3.

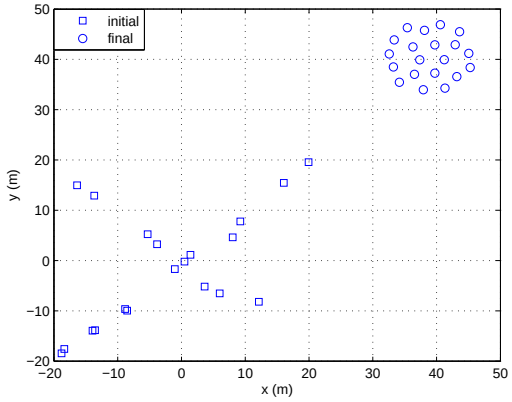

Figure 12. Locations of each MAV in x-y plane at $t = 0$ sec and $t = 80$ sec in Case 4.

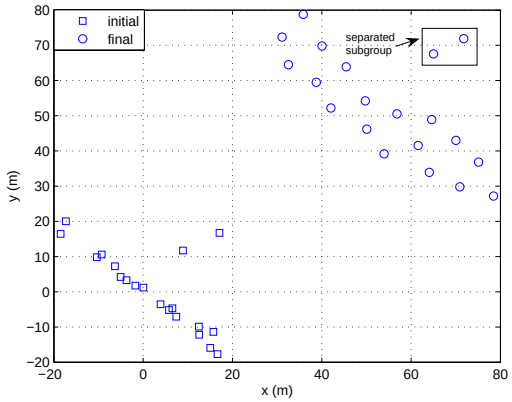

Figure 13. Locations of each MAV in x-y plane at $t = 0$ sec and $t = 80$ sec in Case 5.

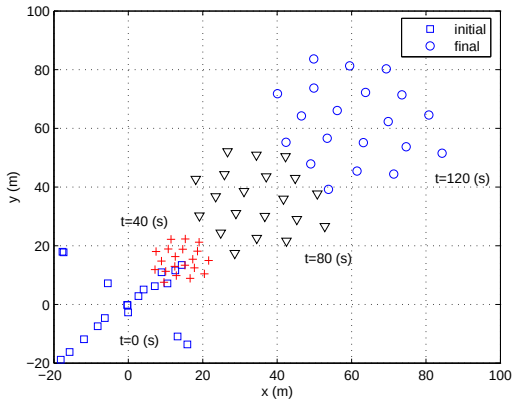

Figure 14. Locations of each MAV in x-y plane at $t = 0, 40, 80, 120$ sec in Case 6